

Ultrafast laser-induced magneto-optical response of CoFeB/MgO/CoFeB magnetic tunneling junction

Cite as: Appl. Phys. Lett. **122**, 111104 (2023); <https://doi.org/10.1063/5.0141071>

Submitted: 02 January 2023 • Accepted: 02 March 2023 • Published Online: 14 March 2023

Bingyu Ji,  Zuanming Jin, Guanjie Wu, et al.



[View Online](#)



[Export Citation](#)



[CrossMark](#)



Time to get excited.
Lock-in Amplifiers – from DC to 8.5 GHz

[Find out more](#)

 Zurich Instruments

Ultrafast laser-induced magneto-optical response of CoFeB/MgO/CoFeB magnetic tunneling junction

Cite as: Appl. Phys. Lett. **122**, 111104 (2023); doi: [10.1063/5.0141071](https://doi.org/10.1063/5.0141071)

Submitted: 2 January 2023 · Accepted: 2 March 2023 ·

Published Online: 14 March 2023






View Online



Export Citation



CrossMark

Bingyu Ji,¹ Zuanming Jin,^{1,a)}  Guanjie Wu,² Jugeng Li,³ Caihua Wan,⁴ Xiufeng Han,⁴  Zongzhi Zhang,² Guohong Ma,³ Yan Peng,¹  and Yiming Zhu¹

AFFILIATIONS

¹Terahertz Technology Innovation Research Institute, Terahertz Spectrum and Imaging Technology Cooperative Innovation Center, Shanghai Key Lab of Modern Optical System, University of Shanghai for Science and Technology, Shanghai 200093, China

²Shanghai Engineering Research Center of Ultra-Precision Optical Manufacturing and Key Laboratory of Micro and Nano Photonic Structures (MOE), School of Information Science and Technology, Fudan University, Shanghai 200433, China

³Department of Physics, Shanghai University, 99 Shangda Road, Shanghai 200444, China

⁴Beijing National Laboratory for Condensed Matter Physics, Institute of Physics, University of Chinese Academy of Sciences, Chinese Academy of Sciences, Beijing 100190, China

^{a)} Author to whom correspondence should be addressed: physics_jzm@usst.edu.cn

ABSTRACT

Understanding of ultrafast spin dynamics is crucial for future ultrafast and energy efficient magnetic memory and storage applications. We study the ultrafast laser-induced magneto-optical response of a CoFeB/MgO/CoFeB magnetic tunneling junction (MTJ), when exciting with a short laser pulse, as a function of magnetic configuration and pump fluence. The ultrafast magnetization of the MTJ drops rapidly in the timescale of 0.33–0.37 ps, which is driven by both electron-spin scattering and spin transport mutually. Subsequently, the energy from the electron and spin reservoirs transfers into the lattice with the timescale of 1.5–2.0 and 5.0–15.0 ps through the electron-phonon and spin-phonon interactions, respectively. Our results suggest that the interfacial spin-orientation of CoFeB/MgO/CoFeB could modulate the interaction constant between spins and phonons. These findings provide insight into the role of MTJ interface in spin dynamics, which will be helpful for opto-spintronic tunnel junction stack designs and applications.

Published under an exclusive license by AIP Publishing. <https://doi.org/10.1063/5.0141071>

The demand for ever faster and energy-efficient data processing has continuously fueled fundamental research on spintronic technology, such as faster data storage, memory, and processing.^{1,2} The ultra-short optical pulses on sub-picosecond timescale present the capability to probe and manipulate the dynamics of magnetization,^{3,4} by using the time-resolved magneto-optical Kerr effect (TRMOKE).^{5,6} The key scientific issues on ultrafast spintronics are related to physical mechanisms, material exploration, and device fabrication.^{7,8}

The typical ultrafast demagnetization process was demonstrated on the Ni film in 1996.⁹ The magnetization of 3d ferromagnets can be optically quenched within 50–300 fs induced by a linear polarization laser pulse and then followed by a slower magnetization recovery on picosecond timescales.^{10–12} When the electrons in the magnetic metal are rapidly heated with an optical pulse, the material undergoes exchange processes of energy and angular momentum between electron, spin, and phonon degrees-of-freedom.^{13–15} The ultrafast demagnetization can further trigger an ultrafast out of equilibrium state. An

enormous variety of complex phenomena in different material systems has been investigated,^{16–20} including coherent precession of the magnetization,^{21,22} laser induced magnetic phase transitions,^{23,24} and all-optical helicity dependent switching.^{25,26}

A super-diffusive spin transport model has been proposed to interpret the ultrafast demagnetization by majority spins away from the excitation region in magnetic multilayers.^{27–31} Among these attempts, Rudolf *et al.* demonstrated that the super-diffusion of excited majority spin electrons from the Ni layer through Ru into the Fe layer can increase or decrease the magnetization of Fe transiently.³² Eschenlohr *et al.* reported that the demagnetization through a hot electron current is as efficient as that created through a direct laser irradiation in Au/Ni/Pt and Pt/Ni/Pt, which can be reproduced by the super-diffusive transport model.³³ Jiang *et al.* demonstrated that the ultrafast enhancement and optical control of magnetization in $L1_0$ -MnGa/GaAs layered structures via super-diffusive spin transports.³⁴

More interesting phenomena were observed as the TRMOKE technique was used to investigate giant magnetoresistance (GMR) structures and magnetic tunnel junction (MTJ).^{35,36} Malinowski *et al.* demonstrated that the interlayer transfer of spin angular momentum in $[\text{Co}/\text{Pt}]_n$ multilayers speed up the demagnetization process when the magnetic configuration is antiparallel.³⁵ He *et al.* observed that the ultrafast demagnetization can be engineered by the hot electrons tunneling.³⁶ It was pointed out that these works focused mainly on the speed and magnitude of the ultrafast demagnetization. However, the timescale of energy exchange between electron, spin, and lattice associated with the spin-flip and spin-transport is still far from conclusive.

In this Letter, we present a laser-induced magneto-optical response of a realistic MTJ device, by performing TRMOKE measurements as a function of magnetic configuration and pump fluence. The demagnetization dynamics are qualitatively similar to those of CoFeB/MgO/CoFeB³⁶ and common 3d ferromagnet.^{4,37,38} In the ultrafast magnetization relaxation, it was observed that the electron-phonon coupling does not change for both antiparallel (AP) state and parallel (P) state of the magnetizations between two FM layers. While, the time constant of spin-phonon interaction increases at P state in comparison with the AP state, which demonstrates that the interfacial spin-orientation could play a role in the spin-phonon coupling. The investigation of the coupling between spin, electron, and lattice in a strongly out-of-equilibrium regime is required for ultrafast magnetism and data recording technology.

The MTJ sample ($10 \times 10 \text{ mm}^2$) used in the experiment has a multi-stack of Ta(20)/Co₂₀Fe₆₀B₂₀(1.2)/MgO(5)/Co₂₀Fe₆₀B₂₀(1.7)/Ta(0.25)/Co(1.4)/Pt(0.8)/[Co(0.3)/Pt(0.8)]₃/Co(0.6)/Ru(0.85)/Co(0.6)/Pt(0.8)/[Co(0.3)/Pt(0.8)]₉/Ta(5)/Ru(6), which was deposited on the thermally oxidized Si wafer, as shown in Fig. 1(a). The numbers are thicknesses in nanometers (nm). First, a 20 nm Ta seed layer was deposited on a thermally oxidized Si substrate. Then, the core MTJ structure of CoFeB(1.2)/MgO(5)/CoFeB(1.7) was deposited by magnetron sputtering

with a base pressure of $4 \times 10^{-6} \text{ Pa}$. The synthetic antiferromagnetic (SAF) layer Co(1.4)/Pt(0.8)/[Co(0.3)/Pt(0.8)]₃/Co(0.6)/Ru(0.85)/Co(0.6)/Pt(0.8)/[Co(0.3)/Pt(0.8)]₉ was deposited on the CoFeB/MgO/CoFeB. The spin orientation of the CoFeB FM1 layer is “pinned” by the exchange bias between the net interfacial moment of the FM1 layer and the SAF layer. Finally, a 5 nm Ta and a 6 nm Ru layers were covered to protect the MTJ against oxidation. The sample was then annealed at 350 °C in a vacuum chamber for an hour. Argon was used as the sputtering gas. The MTJ multi-stacks are in out-of-plane vertical AP state without external magnetic field. The magnetic properties of the sample were characterized by vibrating sample magnetometer (VSM) with an external field applied perpendicularly to the surface. The tunneling magnetoresistance of the MTJ multi-stack was measured up to 150% at room temperature, by using a DC four-probe method with a 3D Helmholtz coil system.

The laser-induced dynamic magneto-optical properties of the MTJ multi-stack were measured using the TRMOKE technique based on a conventional pump-probe setup, as shown in Fig. 1(b). The MTJ multi-stack was irradiated with unfocused laser pulses from a Ti:sapphire laser amplifier with the center wavelength of 800 nm (photon-energy of 1.55 eV), the pulse duration of 150 fs, and the repetition rate of 1 kHz. The laser beam was split into pump and probe beams by a beam splitter. The spin and charge dynamic behaviors were launched by an intense p-polarized pump beam (the beam diameter at the sample is around 2 mm) at around normal incidence. The s-polarized probe beam reflects from the sample surface at an incident angle of about 10°. The beam diameter at the sample was about half as large as that of the pump beam, which guarantees a homogeneous probing region. In addition, the probe fluence was one order of magnitude weaker, such that it did not induce any changes in the sample. Note that the probe pulse averages over its finite duration temporally and penetration volume spatially. The polar Kerr rotation of the reflected probe beam was recorded by an optical balanced bridge and

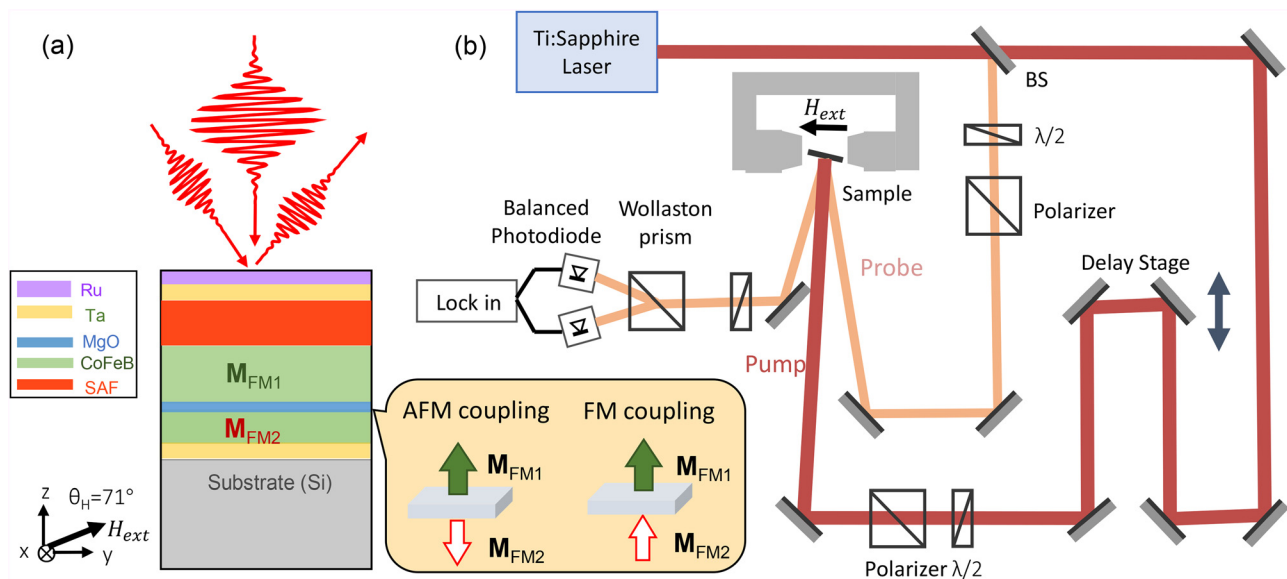


FIG. 1. (a) Schematic illustration of the TRMOKE measurement of the MTJ structure with anti-ferromagnetic (AFM) and ferromagnetic (FM) coupling. (b) Sketch of the TRMOKE experimental setup.

by a lock-in amplifier, which was synchronized to an optical chopper. The chopper modulates the pump beam at a frequency of 108 Hz. A pair of Helmholtz coils (East Changing Technologies, EM 5) generated an external magnetic field \mathbf{H}_{ext} with a maximum value of 2 T. \mathbf{H}_{ext} was tilted at an angle $\theta_{\text{H}} \approx 71^\circ$ to the film normal. All measurements were performed at room temperature.

Figure 2(a) shows the normalized static polar hysteresis loop of the MTJ, as a function of external magnetic field without pump pulse applied. The square loop indicates that the film has perpendicular magnetic anisotropy (PMA). The hysteresis loop is constituted by two minor loops with two distinct switching fields, which are separated by two antiferromagnetic plateaus. The magnetic directions of two CoFeB FM layers can be controlled by the external magnetic field. The switching fields of the top and the bottom CoFeB FM layer are around 290 and 180 mT, respectively. The magnetization directions of both FM1 and FM2 are plotted in Fig. 2(a) for different applied magnetic fields. In our case, $\mathbf{H}_{\text{ext},z} = \pm 500$ mT is sufficient to overcome the high switching field and then in this case the magnetizations of both FM layers are aligned to be parallel with each other.

Figures 2(b) and 2(c) show the pump-induced changes in the TRMOKE signal $\Delta I^{\text{TRMOKE}}(\Delta t)$, which are recorded by a time-delayed probe beam for $\mathbf{H}_{\text{ext},z} = \pm 100$ and ± 500 mT, respectively. It can be found that the $\Delta I^{\text{TRMOKE}}(\Delta t)$ signals depend on both orientation and

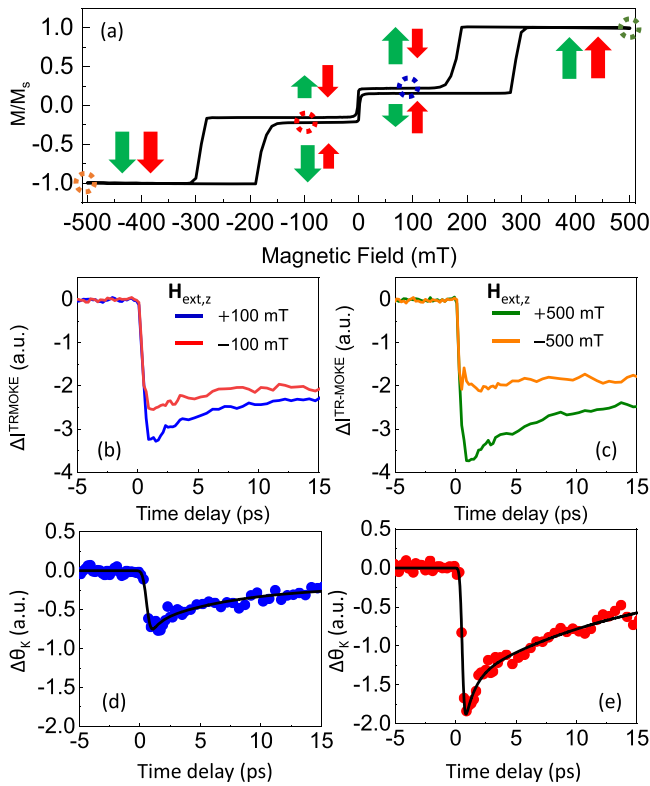


FIG. 2. (a) Perpendicular magnetic hysteresis loop of the MTJ stack. (b) TRMOKE curves for the s-polarized probe beam. The sample is magnetized by (b) $\mathbf{H}_{\text{ext},z} = \pm 100$ and (c) ± 500 mT. The dashed circles in (a) represent the measured states of AP and P. The difference curves of $\Delta\theta_K(\Delta t)$ for the (d) AP and (e) P configurations. The solid lines are the fittings.

magnitude of the external magnetic fields, which means that the penetration depth of the laser beam is larger than the thickness of the capping and SAF layers (29.5 nm) within the sample. Two FM layers first have opposite magnetizations when $\mathbf{H}_{\text{ext},z} = \pm 100$ mT and then they are aligned to be parallel with each other when $\mathbf{H}_{\text{ext},z} = \pm 500$ mT. The $\Delta I^{\text{TRMOKE}}(\Delta t)$ signal drops within ~ 500 fs after the sample's excitation by the pump pulse. The incident fluences are 1.0 and 0.05 mJ cm^{-2} for the pump and probe laser beams, respectively. It can be found that the $\Delta I^{\text{TRMOKE}}(\Delta t)$ curves are not inverted after reversal of the external magnetic fields. Proposed by Kampfrath *et al.*, the $\Delta I^{\text{TRMOKE}}(\Delta t)$ can be expressed by the sum of the magnetic and non-magnetic contributions phenomenologically³⁹

$$\Delta I^{\text{TRMOKE}}(\Delta t) = a_0 \Delta M(\Delta t) + M_0 \Delta a(\Delta t) + \Delta b(\Delta t). \quad (1)$$

The first term of the TRMOKE signal is proportional to the demagnetization dynamics. The second term scales with the static magnetization of the sample M_0 . $\Delta a(\Delta t)$ is caused by pump-induced changes in both the refractive index and the magneto-optical coupling constant. It is reasonable to assume that the reversal of M_0 reverses the pump-induced ΔM . The third term $\Delta b(\Delta t)$ is the ultrafast change in the nonmagnetic TRMOKE signal, which is generally sensitive to the polarization state of the probe beam. To focus on the pure magnetization dependent contributions and eliminating the $\Delta b(\Delta t)$, we considered the pump-induced change in the polar Kerr rotation signal expressed as the difference of $\Delta I^{\text{TRMOKE}}(\Delta t, \pm \mathbf{M})$, changing with the magnetization direction,

$$\begin{aligned} \Delta\theta_K(\Delta t) &= \frac{1}{2} (\Delta I^{\text{TRMOKE}}(\Delta t, +\mathbf{M}) - \Delta I^{\text{TRMOKE}}(\Delta t, -\mathbf{M})) \\ &= a_0 \Delta M(\Delta t) + M_0 \Delta a(\Delta t). \end{aligned} \quad (2)$$

Figures 2(d) and 2(e) show the typical $\Delta\theta_K(\Delta t)$ curves for AP and P states comparatively, induced by a pump pulse at fluence of 1 mJ cm^{-2} . When the pump laser heats the sample, a steep decrease in the magnitude of $\Delta\theta_K(\Delta t)$ is observed in the timescale less than ~ 500 fs. The decrease corresponds to the sub-picosecond quenching of magnetic order in the MTJ multi-stack, which is followed by a subsequent recovery on a longer timescale of several picoseconds. It is possible to achieve a precession of the net magnetization at the frequency of the ferromagnetic resonance, by tuning the orientation and the strength of the applied magnetic field.^{40,41} In our case, there is no signature of the magnetization precession observed for both P and AP states. This is owing to the large PMA to suppress the reorientation of the magnetization. The pump-laser induced $\Delta\theta_K(\Delta t)$ curves can be used to depict the ultrafast time evolution of changes in both the out-of-plane magnetization component and magneto-optical coupling constant in the MTJ multi-stack.

To quantify the results of $\Delta\theta_K(\Delta t)$, we employ a phenomenological double exponential model to fit the raw $\Delta\theta_K(\Delta t)$ data⁴²

$$\begin{aligned} \Delta\theta_K(\Delta t) &= C(t) \otimes \left\{ \left[1 - e^{-\frac{\Delta t}{\tau_{\text{dem}}}} \right] \right. \\ &\quad \left. \times \left(A \times e^{-\frac{\Delta t}{\tau_{e-ph}}} + B \times e^{-\frac{\Delta t}{\tau_{s-ph}}} \right) \right\} + D, \end{aligned} \quad (3)$$

where τ_{dem} is defined as the sub-picosecond time constant to reach the minimum of magnetization, which indicates how fast the photoinduced demagnetization is. τ_{e-ph} and τ_{s-ph} are two time-constants of

the exponential recovery of magnetization. A and B are amplitudes of the relaxation behavior of ultrafast demagnetization. D is a baseline. $C(t)$ is a cross-correlation function of pump and probe pulses. Symbol \otimes denotes the operation of convolution. Equation (3) is used to fit the data of $\Delta\theta_K(\Delta t)$, as shown by the solid lines in Figs. 2(d) and 2(e). First, one can see that τ_{dem} are 0.46 ± 0.09 and 0.31 ± 0.04 ps for AP and P states, respectively. It should be noted that it is hard to distinguish the difference of τ_{dem} by one single measurement with the error bars. Decreasing the magnetization implies increasing the spin disorder and, thus, the spin temperature. Second, we would like to stress that τ_{e-ph} and τ_{s-ph} are attributed to the time constants of electron-phonon and spin-phonon couplings, accordingly, which indicate different mechanisms responsible for the relaxation of magnetization.^{43–46} They quantify energy transfer dynamics from electron and spin subsystems to lattice subsystem. The lattice interacts with the spin as a reservoir of dissipated angular momentum from spin system.⁴⁷ Finally, after about tens of picoseconds, the temperatures of electron, spin, and lattice subsystems are equilibrated, and then the whole excited area will cool down on the timescale of heat transfer into the substrate at room temperature.

It is known that the magnetization dynamics can be controlled by changing the pump fluence. In order to gain insight into the dynamical electron-phonon and spin-phonon interactions in the MTJ after laser excitation, $\Delta\theta_K(\Delta t)$ measurements with different pump fluences ranging from 0.2 to 1.8 mJ cm^{-2} were performed. Figures 3(a) and 3(b) show the temporal dynamics of $\Delta\theta_K(\Delta t)$ for various pump fluences, applied with $H_{ext,z} = \pm 100$ and ± 500 mT, respectively. It can be seen that the peak amplitude of $\Delta\theta_K(\Delta t)$ is roughly proportional to the pump fluence, as shown in Figs. 3(c) and 3(d). This means that a larger

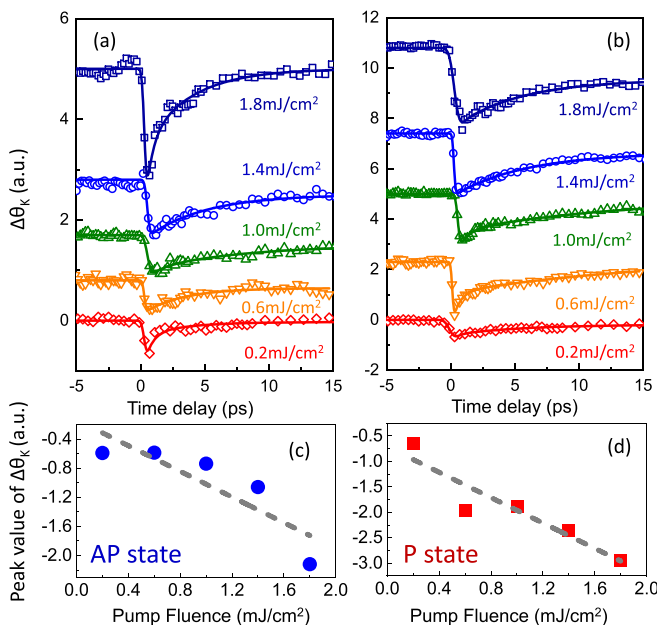


FIG. 3. The ultrafast laser-induced magneto-optical signal $\Delta\theta_K(\Delta t)$ obtained in (a) AP and (b) P state. For clarity, the baselines in (a) and (b) are shifted vertically. Pump fluence dependences of the demagnetization amplitudes in (c) AP and (d) P states.

pump fluence results in a larger degree of sub-picosecond demagnetization amplitude. Fitting the measurement data using Eq. (3) enables us to extract the characteristic demagnetization time τ_{dem} , electron-phonon interaction, and spin-phonon interaction time constants of τ_{e-ph} and τ_{s-ph} , which are summarized in Figs. 4(a)–4(c).

First, as shown in Fig. 4(a), the extracted τ_{dem} of our MTJ stack is largely not dependent on the pump fluence. The pump fluence independent mean value of $\tau_{dem} = 0.33 \pm 0.09$ s and $\tau_{dem} = 0.37 \pm 0.10$ ps for the AP and P states, respectively. Although the ultrafast demagnetization dynamics of the P and AP states are very similar, the ultrafast spin-transport between two CoFeB layers by the tunneling of hot electrons through the MgO barrier cannot be excluded during the timescale of demagnetization. The reasons are mainly as following. From a previous experimental study, Carpena *et al.* attributed the ultrafast demagnetization in Fe to the electron-spin scattering.⁴⁸ It is, therefore, reasonable to expect that the time constant of electron-spin interaction is proportional to the electron's peak temperature (pump fluence). In contrast, the measured τ_{dem} in our MTJ multi-stack is not dependent on the pump fluence, indicating that the electron-spin scattering is not the whole mechanism for the ultrafast demagnetization. From a recent theoretical study, Ashok *et al.* found that, as compared to the case without transport, the linear correlation between the quenching time and quenching magnitude in the case with transport is weakened,⁴⁹ which is in line with our observations. It should be noted that the terahertz spectroscopy has become a complementary technique to demonstrate the spin transport dynamics.^{50–56}

Second, as shown in Fig. 4(b), the time constant of the electron-phonon interaction is around $\tau_{e-ph} \sim 1.5$ –2.0 ps. We find that a maximum value is reached with the pump fluence of 1.4 mJ cm^{-2} . This behavior is consistent with the findings observed in Pt/Co₂FeAl_{0.5}Si_{0.5}⁴² and YMnO₃ film,⁵⁷ which can be attributed to the divergence of spin heat capacity in both the FM layer and multiferroic materials. The diverging behavior of τ_{e-ph} can be used to indicate the pump fluence at which the Curie temperature of the MTJ is reached.

Finally, Fig. 4(c) shows that the time constant of the spin-phonon interaction is around $\tau_{s-ph} \sim 5$ –15 ps, which is consistent with the timescale of coherent acoustic phonons that modulated the exchange interaction in Fe, observed by terahertz emission spectroscopy.⁵⁸ It can be found that $\tau_{s-ph} = 11.1 \pm 4.2$ ps for the P state is enhanced by two times compared with 4.5 ± 1.5 ps for the AP state, below the pump fluence of 1.4 mJ cm^{-2} . This observation suggests that the interaction between spins scattering/spin tunneling and phonon modes at the interfaces of FM1/MgO/FM2 is stronger in AP state than that in P state, leading to a faster decay of the spin temperature in the AP state. While, for the pump fluence above ~ 1.4 mJ cm^{-2} , the τ_{s-ph} becomes similar for both P and AP states because the whole system reaches paramagnetic state transiently.

To conclude, an optical pump-probe technique was used to measure the time-resolved magneto-optical response of a realistic MTJ multi-stack with PMA at room temperature. Our results provide a dynamic information of energy redistribution for electrons, spins, and phonons in an MTJ device upon laser excitation. The ultrafast demagnetization is attributed to a driving force from both electron-spin scattering and spin transport mutually. We have observed that the electron-phonon interaction is modified by the magnetic heat capacity divergence. In addition, our results indicate a controllable spin-phonon interaction, depending on the alignment of the magnetizations

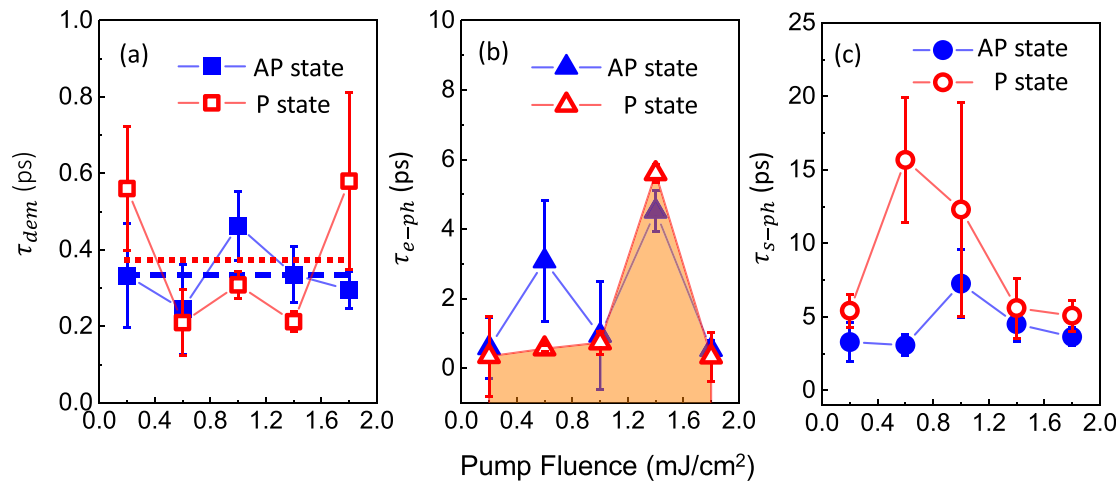


FIG. 4. Time constants of (a) demagnetization τ_{dem} , (b) electron-phonon interaction τ_{e-ph} , and (c) spin-phonon interaction τ_{s-ph} , extracted from fits as functions of pump fluences.

in two FM layers. These physical effects could have profound implications regarding realization and optimization of the device functionalities in opto-spintronic tunnel junctions.^{59,60}

This work was supported by the National Natural Science Foundation of China (NSFC, Grant Nos. 61975110, 61988102, 61735010, 11874120, and 52171230); the 111 Project (Grant No. D18014); the National Key Research and Development Program (No. 2022YFA1404004); the Key Domestic Scientific and Technological Cooperation projects in Shanghai (No. 21015800200); the Key project supported by Science and Technology Commission Shanghai Municipality (Grant No. YDZX20193100004960); the Science and Technology Commission of Shanghai Municipality (No. 22JC1400200); the Science and Technology Commission of Shanghai Municipality (Shanghai Rising-Star Program Grant No. 18QA1401700); and the Shanghai Educational Development Foundation (Grant No. 16CG45). C.H.W. appreciates the financial support from Youth Innovation Promotion Association, CAS (No. 2020008).

AUTHOR DECLARATIONS

Conflict of Interest

The authors have no conflicts to disclose.

Author Contributions

Bingyu Ji: Data curation (lead); Methodology (lead); Project administration (lead); Writing – original draft (equal). **Yiming Zhu:** Conceptualization (equal); Funding acquisition (equal); Investigation (equal); Project administration (equal); Resources (equal); Supervision (equal); Writing – review & editing (equal). **Zuanming Jin:** Conceptualization (lead); Data curation (lead); Formal analysis (lead); Funding acquisition (lead); Investigation (lead); Methodology (lead); Project administration (lead); Resources (lead); Software (lead); Supervision (lead); Validation (lead); Visualization (lead); Writing – original draft (lead); Writing – review & editing (lead). **Guanjie Wu:** Data curation (equal); Formal analysis (equal); Investigation (equal);

Methodology (equal); Writing – original draft (equal). **Jugeng Li:** Data curation (equal); Formal analysis (equal); Investigation (equal); Methodology (equal); Writing – original draft (equal). **Caihua Wan:** Conceptualization (equal); Funding acquisition (equal); Investigation (equal); Methodology (equal); Project administration (equal); Resources (equal); Writing – original draft (equal); Writing – review & editing (equal). **Xiufeng Han:** Conceptualization (equal); Formal analysis (equal); Funding acquisition (equal); Investigation (equal); Project administration (equal); Resources (equal); Supervision (equal); Writing – review & editing (equal). **Zongzhi Zhang:** Conceptualization (equal); Investigation (equal); Project administration (equal); Resources (equal); Supervision (equal); Writing – original draft (equal); Writing – review & editing (equal). **Guohong Ma:** Investigation (equal); Project administration (equal); Resources (equal); Writing – original draft (equal); Writing – review & editing (equal). **Yan Peng:** Conceptualization (equal); Investigation (equal); Resources (equal); Software (equal); Supervision (equal); Writing – original draft (equal); Writing – review & editing (equal).

DATA AVAILABILITY

The data that support the findings of this study are available from the corresponding author upon reasonable request.

REFERENCES

- ¹C. Chappert, A. Fert, and F. N. V. Dau, “The emergence of spin electronics in data storage,” *Nat. Mater.* **6**, 813–823 (2007).
- ²N. Jones, “How to stop data centres from gobbling up the world’s electricity,” *Nature* **561**, 163 (2018).
- ³A. Kirilyuk, A. V. Kimel, and T. Rasing, “Ultrafast optical manipulation of magnetic order,” *Rev. Mod. Phys.* **82**, 2731 (2010).
- ⁴B. Koopmans, G. Malinowski, F. Dalla Longa, D. Steiauf, M. Fähnle, T. Roth, M. Cinchetti, and M. Aeschlimann, “Explaining the paradoxical diversity of ultrafast laser induced demagnetization,” *Nat. Mater.* **9**, 259 (2010).
- ⁵G. M. Muller, J. Walowski, M. Djordjevic, G.-X. Miao, A. Gupta, A. V. Ramos, K. Gehrke, V. Moshnyaga, K. Samwer, J. Schmalhorst, A. Thomas, A. Hutten, G. Reiss, J. S. Moodera, and M. Munzenberg, “Spin polarization in half-metals probed by femtosecond spin excitation,” *Nat. Mater.* **8**, 56 (2009).

- ⁶Q. L. Ma, S. Iihama, X. M. Zhang, T. Miyazaki, and S. Mizukami, "Spin dynamics induced by ultrafast heating with ferromagnetic/antiferromagnetic interfacial exchange in perpendicularly magnetized hard/soft bilayers," *Appl. Phys. Lett.* **107**, 222404 (2015).
- ⁷C. Boeglin, E. Beaurepaire, V. Halté, V. López-Flores, C. Stamm, N. Pontius, H. A. Dürr, and J.-Y. Bigot, "Distinguishing the ultrafast dynamics of spin and orbital moments in solids," *Nature* **465**, 458 (2010).
- ⁸S. Wang, C. Wei, Y. Feng, H. Cao, W. Li, Y. Cao, B.-O. Guan, A. Tsukamoto, A. Kirilyuk, A. V. Kimel, and X. Li, "Dual-shot dynamics and ultimate frequency of all-optical magnetic recording on GdFeCo," *Light* **10**, 8 (2021).
- ⁹E. Beaurepaire, J.-C. Merle, A. Daunois, and J.-Y. Bigot, "Ultrafast spin dynamics in ferromagnetic nickel," *Phys. Rev. Lett.* **76**, 4250 (1996).
- ¹⁰J.-Y. Bigot, M. Vomir, and E. Beaurepaire, "Coherent ultrafast magnetism induced by femtosecond laser pulses," *Nat. Phys.* **5**, 515 (2009).
- ¹¹D. Cheskis, A. Porat, L. Szapiro, O. Potashnik, and S. Bar-Ad, "Saturation of the ultrafast laser-induced demagnetization in nickel," *Phys. Rev. B* **72**, 014437 (2005).
- ¹²B. Koopmans, M. van Kampen, J. T. Kohlhepp, and W. J. M. de Jonge, "Ultrafast magneto-optics in nickel: Magnetism or optics," *Phys. Rev. Lett.* **85**, 844 (2000).
- ¹³D. Zahn, F. Jakobs, H. Seiler, T. A. Butcher, D. Engel, J. Vorberger, U. Atxitia, Y. W. Windsor, and R. Ernstorfer, "Intrinsic energy flow in laser-excited 3d ferromagnets," *Phys. Rev. Res.* **4**, 013104 (2022).
- ¹⁴J.-H. Shim, A. A. Syed, C.-H. Kim, K. M. Lee, S.-Y. Park, J.-R. Jeong, D.-H. Kim, and D. E. Kim, "Ultrafast giant magnetic cooling effect in ferromagnetic Co/Pt multilayers," *Nat. Commun.* **8**, 796 (2017).
- ¹⁵P. Zhang, Y. Yang, A. Chen, Y. Shi, Y. Wang, L. Du, and D. Ding, "Energy relaxation dynamics in ferromagnetic Co film with femtosecond transient absorption," *Opt. Commun.* **452**, 83–87 (2019).
- ¹⁶S. Alebrand, U. Bierbrauer, M. Hehn, M. Gottwald, O. Schmitt, D. Steil, E. E. Fullerton, S. Mangin, M. Cinchetti, and M. Aeschlimann, "Subpicosecond magnetization dynamics in TbCo alloys," *Phys. Rev. B* **89**, 144404 (2014).
- ¹⁷T. G. H. Blank, S. Hermanussen, T. Lichtenberg, T. Rasing, A. Kirilyuk, B. Koopmans, and A. V. Kimel, "Laser-induced transient anisotropy and large amplitude magnetization dynamics in a Gd/FeCo multilayer," *Adv. Mater. Interfaces* **9**, 2201283 (2022).
- ¹⁸X. Lu, G. Li, Y. Gong, X. Ruan, Y. Yan, Y. Li, L. He, J. Du, V. K. Lazarov, J. Wu, R. Zhang, and Y. Xu, "Sub-100 femtosecond time scale spin dynamics in epitaxial Fe₃O₄ thin film," *Appl. Surf. Sci.* **572**, 151456 (2022).
- ¹⁹T. Jiang, X. Zhao, Z. Chen, Y. You, T. Lai, and J. Zhao, "ultrafast dynamics of demagnetization in FeMn/MnGa bilayer nanofilm structures via phonon transport," *Nanomaterials* **12**, 4088 (2022).
- ²⁰A. R. Will-Cole, C. Wang, N. Bhattacharjee, Y. Liu, and N. X. Sun, "Electric field tuning of ultrafast demagnetization in a magnetoelectric heterostructure," *Phys. Rev. B* **106**, 174401 (2022).
- ²¹G. Wu, S. Chen, S. Lou, Y. Liu, Q. Y. Jin, and Z. Zhang, "Annealing effect on laser-induced magnetization dynamics in Co/Ni-based synthetic antiferromagnets with perpendicular magnetic anisotropy," *Appl. Phys. Lett.* **115**, 142402 (2019).
- ²²Z. Zhu, G. Wu, Y. Ren, S. Lou, Q. Y. Jin, and Z. Zhang, "Modulation of magnetic damping in antiferromagnet/CoFeB heterostructures," *Appl. Phys. Lett.* **116**, 182407 (2020).
- ²³D. Huang, D. Lattery, and X. Wang, "Materials engineering enabled by time-resolved magneto-optical Kerr effect for spintronic applications," *ACS Appl. Electron. Mater.* **3**, 119–127 (2021).
- ²⁴C. Wang and Y. Liu, "Ultrafast optical manipulation of magnetic order in ferromagnetic materials," *Nano Convergence* **7**, 35 (2020).
- ²⁵C. D. Stanciu, F. Hansteen, A. V. Kimel, A. Kirilyuk, A. Tsukamoto, A. Itoh, and T. Rasing, "All-optical magnetic recording with circularly polarized light," *Phys. Rev. Lett.* **99**, 047601 (2007).
- ²⁶A. V. Kimel and M. Li, "Writing magnetic memory with ultrashort light pulses," *Nat. Rev. Mater.* **4**, 189 (2019).
- ²⁷M. Battiato, K. Carva, and P. M. Oppeneer, "Superdiffusive spin transport as a mechanism of ultrafast demagnetization," *Phys. Rev. Lett.* **105**, 027203 (2010).
- ²⁸M. Battiato, K. Carva, and P. M. Oppeneer, "Theory of laser-induced ultrafast superdiffusive spin transport in layered heterostructures," *Phys. Rev. B* **86**, 024404 (2012).
- ²⁹M. Beens, R. A. Duine, and B. Koopmans, "Modeling ultrafast demagnetization and spin transport: The interplay of spin-polarized electrons and thermal magnons," *Phys. Rev. B* **105**, 144420 (2022).
- ³⁰R. Rouzegar, L. Brandt, L. Nádvorník, D. A. Reiss, A. L. Chekhov, O. Gueckstock, C. In, M. Wolf, T. S. Seifert, P. W. Brouwer, G. Woltersdorf, and T. Kampfrath, "Laser-induced terahertz spin transport in magnetic nanostructures arises from the same force as ultrafast demagnetization," *Phys. Rev. B* **106**, 144427 (2022).
- ³¹P. Scheid, Q. Remy, S. Lebègue, G. Malinowski, and S. Mangin, "Light induced ultrafast magnetization dynamics in metallic compounds," *J. Magn. Magn. Mater.* **560**, 169596 (2022).
- ³²D. Rudolf, C. La-o-vorakiat, M. Battiato, R. Adam, J. M. Shaw, E. Turgut, P. Maldonado, S. Mathias, P. Grychtol, H. T. Nembach, T. J. Silva, M. Aeschlimann, H. C. Kapteyn, M. M. Murnane, C. M. Schneider, and P. M. Oppeneer, "Ultrafast magnetization enhancement in metallic multilayers driven by superdiffusive spin current," *Nat. Commun.* **3**, 1037 (2012).
- ³³A. Eschenlohr, M. Battiato, P. Maldonado, N. Pontius, T. Kachel, K. Holldack, R. Mitzner, A. Föhlisch, P. M. Oppeneer, and C. Stamm, "Ultrafast spin transport as key to femtosecond demagnetization," *Nat. Mater.* **12**, 323 (2013).
- ³⁴T. Jiang, X. Zhao, Z. Chen, Y. You, T. Lai, and J. Zhao, "Ultrafast enhancement and optical control of magnetization in ferromagnet/semiconductor layered structures via superdiffusive spin transports," *Mater. Today Phys.* **26**, 100723 (2022).
- ³⁵G. Malinowski, F. D. Longa, J. H. H. Rietjens, P. V. Paluskar, R. Huijink, H. J. M. Swagten, and B. Koopmans, "Control of speed and efficiency of ultrafast demagnetization by direct transfer of spin angular momentum," *Nat. Phys.* **4**, 855–858 (2008).
- ³⁶W. He, T. Zhu, X. Q. Zhang, H. T. Yang, and Z. H. Cheng, "Ultrafast demagnetization enhancement in CoFeB/MgO/CoFeB magnetic tunneling junction driven by spin tunneling current," *Sci. Rep.* **3**, 2883 (2013).
- ³⁷J. Güdde, U. Conrad, V. Jéahnke, J. Hohlfeld, and E. Matthias, "Magnetization dynamics of Ni and Co films on Cu(001) and of bulk nickel surfaces," *Phys. Rev. B* **59**, R6608 (1999).
- ³⁸I. Radu, K. Vahaplar, C. Stamm, T. Kachel, N. Pontius, H. A. Dürr, T. A. Ostler, J. Barker, R. F. L. Evans, R. W. Chantrell, A. Tsukamoto, A. Itoh, A. Kirilyuk, T. Rasing, and A. V. Kimel, "Transient ferromagnetic-like state mediating ultrafast reversal of antiferromagnetically coupled spins," *Nature* **472**, 205–208 (2011).
- ³⁹T. Kampfrath, R. G. Ulbrich, F. Leuenberger, M. Munzenberg, B. Sass, and W. Felsch, "Ultrafast magneto-optical response of iron thin films," *Phys. Rev. B* **65**, 104429 (2002).
- ⁴⁰G. Wu, Y. Ren, Q. Jin, and Z. Zhang, "Temperature-dependent magnetization dynamics in nanoscale Cu(t_{Cu})/[Co/Ni]_N perpendicular multilayers: implications for spintronic applications," *ACS Appl. Nano Mater.* **3**, 11555 (2020).
- ⁴¹S. Chen, G. Wu, Q. Xie, J. Zhou, X. Shu, Z. Zhang, and J. Chen, "Investigation of spin transport properties in perpendicularly magnetized MoS₂/Pt/[Co/Ni]_n multilayers with effective spin injection into two-dimensional MoS₂," *Phys. Rev. Appl.* **14**, 014095 (2020).
- ⁴²J. Besbas, L. M. Loong, Y. Wu, and H. Yang, "The role of Pt underlayer on the magnetization dynamics of perpendicular magnetic anisotropy, Pt/Co₂FeAl_{0.5}Si_{0.5}/MgO," *Appl. Phys. Lett.* **108**, 232408 (2016).
- ⁴³R. Wilks, R. J. Hicken, M. Ali, B. J. Hickey, J. D. R. Buchanan, A. T. G. Pym, and B. K. Tanner, "Investigation of ultrafast demagnetization and cubic optical nonlinearity of Ni in the polar geometry," *J. Appl. Phys.* **95**, 7441 (2004).
- ⁴⁴V. V. Kruglyak and R. J. Hicken, "Simple theory of hot electron dynamics observed by femtosecond ellipsometry," *J. Appl. Phys.* **99**, 08P903 (2006).
- ⁴⁵V. V. Kruglyak, R. J. Hicken, P. Matousek, and M. Towrie, "Spectroscopic study of optically induced ultrafast electron dynamics in gold," *Phys. Rev. B* **75**, 035410 (2007).
- ⁴⁶U. Ritzmann, P. M. Oppeneer, and P. Maldonado, "Theory of out-of-equilibrium electron and phonon dynamics in metals after femtosecond laser excitation," *Phys. Rev. B* **102**, 214305 (2020).
- ⁴⁷S. R. Tauchert, M. Volkov, D. Ehberger, D. Kazenwadel, M. Evers, H. Lange, A. Donges, A. Book, W. Kreuzpaintner, U. Nowak, and P. Baum, "Polarized phonons carry angular momentum in ultrafast demagnetization," *Nature* **602**, 73 (2022).

- ⁴⁸E. Carpena, E. Mancini, C. Dallera, M. Brenna, E. Puppini, and S. D. Silvestri, "Dynamics of electron-magnon interaction and ultrafast demagnetization in thin iron films," *Phys. Rev. B* **78**, 174422 (2008).
- ⁴⁹S. Ashok, C. Seibel, S. T. Weber, J. Briones, and B. Rethfeld, "Influence of diffusive transport on ultrafast magnetization dynamics," *Appl. Phys. Lett.* **120**, 142402 (2022).
- ⁵⁰Z. Jin, A. Tkach, F. Casper, V. Spetter, H. Grimm, A. Thomas, T. Kampfrath, M. Bonn, M. Kläui, and D. Turchinovich, "Accessing the fundamentals of magnetotransport in metals with terahertz probes," *Nat. Phys.* **11**, 761 (2015).
- ⁵¹T. Kampfrath, M. Battiato, P. Maldonado, G. Eilers, J. Nötzold, S. Mährlein, V. Zbarsky, F. Freimuth, Y. Mokrousov, S. Blügel, M. Wolf, I. Radu, P. M. Oppeneer, and M. Münzenberg, "Terahertz spin current pulses controlled by magnetic heterostructures," *Nat. Nanotechnol.* **8**, 256 (2013).
- ⁵²M. Shalaby, C. Vicario, and C. P. Hauri, "Low frequency terahertz-induced demagnetization in ferromagnetic nickel," *Appl. Phys. Lett.* **108**, 182903 (2016).
- ⁵³A. L. Chekhov, Y. Behovits, J. J. F. Heitz, C. Denker, D. A. Reiss, M. Wolf, M. Weinelt, P. W. Brouwer, M. Münzenberg, and T. Kampfrath, "Ultrafast demagnetization of iron induced by optical versus terahertz pulses," *Phys. Rev. X* **11**, 041055 (2021).
- ⁵⁴E. A. Mashkovich, K. A. Grishunin, H. Munekata, and A. V. Kimel, "Ultrafast demagnetization of ferromagnetic semiconductor InMnAs by dual terahertz and infrared excitations," *Appl. Phys. Lett.* **117**, 122406 (2020).
- ⁵⁵J. Walowski and M. Münzenberg, "Perspective: Ultrafast magnetism and THz spintronics," *J. Appl. Phys.* **120**, 140901 (2016).
- ⁵⁶Z. Jin, J. Li, W. Zhang, C. Guo, C. Wan, X. Han, Z. Cheng, C. Zhang, A. V. Balakin, A. P. Shkurinov, Y. Peng, G. Ma, Y. Zhu, J. Yao, and S. Zhuang, "Magnetic modulation of terahertz waves via spin-polarized electron tunneling based on magnetic tunnel junctions," *Phys. Rev. Appl.* **14**, 014032 (2020).
- ⁵⁷Z. Jin, H. Ma, G. Li, Y. Xu, G. Ma, and Z. Cheng, "Ultrafast dynamics of the Mn³⁺ d-d transition and spin-lattice interaction in YMnO₃ film," *Appl. Phys. Lett.* **100**, 021106 (2012).
- ⁵⁸W. Zhang, P. Maldonado, Z. Jin, T. S. Seifert, J. Arabski, G. Schmerber, E. Beaurepaire, M. Bonn, T. Kampfrath, P. M. Oppeneer, and D. Turchinovich, "Ultrafast terahertz magnetometry," *Nat. Commun.* **11**, 4247 (2020).
- ⁵⁹L. Wang, H. Cheng, P. Li, Y. L. W. van Hees, Y. Liu, K. Cao, R. Lavrijsen, X. Lin, B. Koopmans, and W. Zhao, "Picosecond optospinronic tunnel junctions," *Proc. Natl. Acad. U. S. A.* **119**, e2204732119 (2022).
- ⁶⁰P. Dey and J. N. Roy, *Opto-Spintronics* (Springer, Singapore, 2021).